Research Square

Preprints are preliminary reports that have not undergone peer review.
They should not be considered conclusive, used to inform clinical practice,
or referenced by the media as validated information.

Integrated In Vitro and In Silico Toxicological Assessment of N-Nitroso Vildagliptin: Redox Dysregulation, DNA Integrity, and Molecular Interactions

Pooja Giri
Dr Vishwanath Karad MIT World Peace University
Anuruddha Rajaram Chabukswar
anuruddha.chabukswar@mitwpu.edu.in

Dr Vishwanath Karad MIT World Peace University

Research Article

Keywords: N-Nitroso vildagliptin, Comet assay, Antioxidant/redox homeostasis, Nitric oxide, Oxidative stress

Posted Date: November 23rd, 2026

DOI: https://doi.org/10.21203/rs.3.rs-11645679/v1

License: This work is licensed under a Creative Commons Attribution 4.0 International License.
Read Full License

Additional Declarations:
No competing interests reported.

Table 1 is available in the Supplementary Files section.

Integrated *In Vitro* and *In Silico* Toxicological Assessment of N-Nitroso Vildagliptin: Redox Dysregulation, DNA Integrity, and Molecular Interactions

Pooja Giri[1], Anuruddha Chabukswar[1*]

[1]Department of Pharmaceutical Sciences, School of Health Sciences and Technology, Dr Vishwanath Karad MIT World Peace University, Kothrud, Pune, India-411038

Corresponding author*:
Dr. Anuruddha Rajaram Chabukswar,
Dr. Viswanath Karad MIT-World Peace University,
Kothrud, Pune, Maharashtra, India- 411038,
e-mail address: anuruddha.chabukswar@mitwpu.edu.in
Phone No - 9881073208

ABSTRACT

N-nitroso vildagliptin (NN-VLD), identified as a nitrosamine drug substance-related impurity, has emerged as a pharmaceutical safety concern. Its cellular effects, particularly its relationship with oxidative and nitrosative stress (OS/NS) and DNA integrity, remain uncharacterized. Therefore, the present study aimed to synthesized and evaluate its cellular effects with particular emphasis on cytotoxicity, oxidative and nitrosative responses, DNA integrity, and potential molecular interactions with Kepa1 receptor and DNA.NN-VLD was synthesized in-house (yield 97%), and its cytotoxicity was evaluated using the MTT assay. We evaluated OS/NS biomarkers, Nuclear factor erythroid 2–related factor 2 (Nrf2) as an antioxidant pathway, and DNA integrity, while molecular docking with Keap1 and DNA was performed to explore potential molecular interactions. NN-VLD produced concentration-dependent cytotoxicity. Decreased superoxide dismutase (50-100µg/mL), catalase (100-125µg/mL), and reduced glutathione (50-100µg/mL) levels, together with increased malondialdehyde (25-125µg/mL), demonstrated impaired antioxidant defence and increased oxidative burden in treated cells. Nrf2 was significantly reduced at higher concentrations (100-125µg/mL), whereas inducible nitric oxide synthase activity was not induced throughout the studied concentrations. Significant changes in % tail DNA and % head DNA were observed only at 125µg/mL, while other comet parameters remained unaffected and showed favourable predicted interactions with Keap1 and DNA. Overall, NN-VLD induces oxidative burden in cells rather than NS, but does not show oxidative DNA damage at the tested concentration.

KEYWORDS: N-Nitroso vildagliptin, Comet assay, Antioxidant/redox homeostasis, Nitric oxide, Oxidative stress

1. INTRODUCTION

Nitrosamines (NAs) are a class of chemical compounds of toxicological concern because several members possess mutagenic, genotoxic, and carcinogenic properties. Humans can be exposed to nitrosamines through various environmental and dietary sources, and these compounds can also form endogenously under appropriate nitrosating conditions (*1*). In particular, the emergence of nitrosamine drug substance-related impurities (NDSRIs) in pharmaceutical products has raised significant toxicological concern because nitrosation of drug-derived amine functionalities can generate structurally diverse compounds with potentially different biological activities from those of their parent active pharmaceutical ingredients (APIs) and conventional small-molecule nitrosamines (*2*). Importantly, the toxicological behavior of an NDSRI cannot be reliably inferred solely from the established safety profile of its parent drug or from structurally related nitrosamines, as structural differences may influence cellular toxicity, oxidative responses, and DNA-damage potential. Therefore, experimental characterization of individual NDSRIs is essential to define their compound-specific cellular effects and underlying toxicological mechanisms.

Vildagliptin is a widely used dipeptidyl peptidase-4 inhibitor containing a nitrosatable amine functionality (*3,4*), making the formation of N-nitroso vildagliptin (NN-VLD) a relevant pharmaceutical safety concern. Although NN-VLD has been identified and analytically characterized (*5*), its direct cellular toxicological profile remains insufficiently defined. A recent study of the structurally related N-nitroso vildagliptin amide impurity (NNVI) reported concentration-dependent cytotoxicity, alterations in antioxidant defenses, lipid peroxidation, and DNA damage in BALB/3T3 cells (*6*). However, these findings cannot be directly extrapolated to NN-VLD because the two impurities differ structurally and were evaluated in different cellular models. Therefore, compound-specific investigations are needed to assess NN-VLD's direct cellular effects, particularly its influence on redox homeostasis and DNA integrity.

Reactive oxygen species (ROS) are continuously generated during normal cellular metabolism and are controlled by an integrated antioxidant defense system. Superoxide dismutase (SOD) and catalase (CAT) constitute important enzymatic antioxidant defenses, whereas reduced glutathione (rGSH) represents a major non-enzymatic component of cellular redox protection (*7,8*). Excessive ROS generation or insufficient antioxidant capacity can disrupt redox homeostasis and promote oxidative damage to cellular lipids, proteins, and DNA, which might cause cancer (*9*). In parallel, nitric oxide (NO), generated primarily by nitric oxide synthases (NOS), can react with superoxide to form peroxynitrite, a highly reactive nitrogen species that

can contribute to nitrosative cellular injury (*10*). Experimental studies in HepG2 cells show that exposure to conventional nitrosamines, including N-nitrosodimethylamine (NDMA), N-nitrosodiethylamine (NDEA), and N-nitrosomorpholine (NMOR), increases intracellular ROS and induces DNA damage, while antioxidant treatment attenuates these effects (*11,12*). These findings provide a biological rationale for investigating oxidative imbalance as a potential component of NN-VLD-associated cellular injury. The kelch-like ECH-associated protein 1-Nuclear factor erythroid 2- related factor 2 (Keap1-Nrf2) pathway is a key cellular defense mechanism against oxidative stress (OS). Nrf2 regulates the expression of multiple antioxidant and detoxification genes and helps restore redox balance after oxidative injury(*13*). Previous studies have also linked alterations in OS and Nrf2 signalling with cellular and genotoxic responses following nitrosamine exposure (*14*). Inducible nitric oxide synthase (iNOS) is an important enzyme involved in nitric oxide (NO) production, catalyzing the conversion of L-arginine to NO and L-citrulline. Under cellular stress, increased iNOS expression may alter NO availability and contribute to nitrosative stress (*15,16*). Therefore, assessing antioxidant defenses, lipid peroxidation, Nrf2 signalling, and iNOS expression together can provide complementary information on oxidative and nitrosative cellular responses to NN-VLD exposure.

Although metabolic activation contributes to the toxicity of several conventional nitrosamines, the magnitude and biological consequences of such activation vary among individual compounds. Studies using nitrosamines in HepG2 cells have demonstrated that cellular metabolic capacity can influence their DNA-damaging responses (*17*). However, this study aimed to investigate the direct cellular response to NN-VLD exposure, rather than characterize its metabolic activation or identify specific reactive metabolites

Despite growing attention to NDSRI-related pharmaceutical safety, the integrated relationship between direct NN-VLD exposure, cytotoxicity, antioxidant defesce status, lipid peroxidation, Nrf2/iNOS responses, and DNA integrity has not yet been studied. Therefore, this study aimed to provide an integrated toxicological characterization of NN-VLD by evaluating cytotoxicity, enzymatic and non-enzymatic antioxidant defences (SOD, CAT, and rGSH), lipid peroxidation (MDA), Nrf2 and iNOS responses, and DNA integrity in HepG2 cells. We performed molecular docking with DNA and Keap1 to explore potential NN-VLD interactions with these targets. Collectively, this approach assessed whether direct NN-VLD exposure disrupted cellular redox homeostasis and whether these alterations coincided with changes in DNA integrity.

2. MATERIALS AND METHODS

2.1 Chemicals

The reference standard NN-VLD was synthesised in-house by a green approach. Vildagliptin (VLD) was received as a gift sample from Chemicea Pharmaceutical Pvt. Ltd. (Mumbai, India). All chemicals used throughout the study including, acetic acid, Trypsin, Dulbecco's Modified Eagle Medium (DMEM), Fetal Bovine Serum (FBS), Ethylenediaminetetraacetic acid (EDTA), 3-(4,5-dimethylthiazol-2-yl)-2,5-diphenyltetrazolium bromide (MTT), Dimethyl sulfoxide,0.25% Trypsin-EDTA, Nitro Blue Tetrazolium (NBT), Triton X-100 Tetramethoxypropane (TMP), Sodium carbonate (Na_2CO_3) Hydroxylamine hydrochloride, Thiobarbituric acid (TBA), Sodium Dodecyl Sulphate(SDS), Glacial acetic acid(GAA) Hydrogen peroxide (H_2O_2) L-Glutathione reduced, Phosphate Buffer Saline(PBS), Sodium Phosphate (Na_3PO_4), 5,5'-dithiobis-(2-nitrobenzoic acid) (DTNB), sodium nitrite, Low-melting-point agarose (LMA), Normal melting-point agarose (NMA), Tris (hydroxymethyl aminomethane, Ethanol, Ethidium bromide, and Tris-HCl buffer were purches from Merck Life Sciences, sigma Aldrich, Gibco, Thermo Fisher Scientific, HiMedia Laboratories, India and Millipore Sigma.

2.2 Methods

2.2.1 Molecular docking

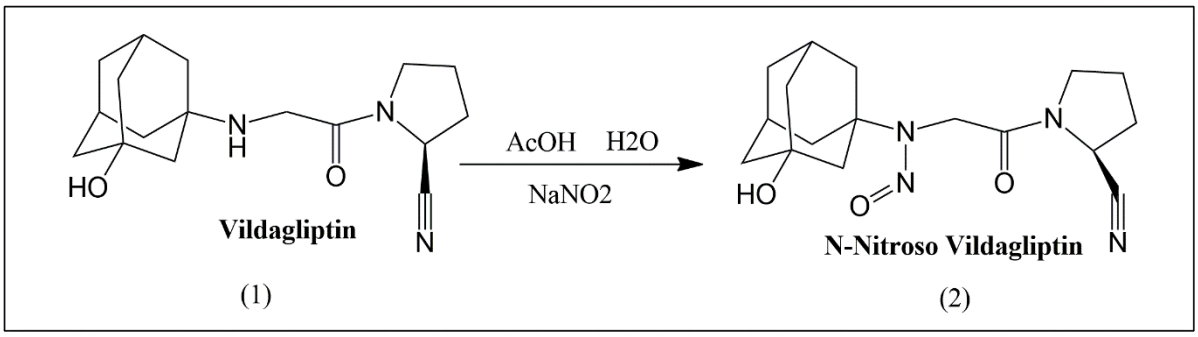
The GeinDock Suite v2.4.1.0 (https://geindock.geinforce.com/,Geinforce Technologies, India) docking tool was employed to perform molecular docking of the ligand with the human Keap1 receptor and co-crystal DNA helix**.** We retrieved the co-crystal DNA helix (PDB ID: 121D) and the Keap1-Nrf2 protein complex (PDB ID: 4L7B) from the RCSB Protein Data Bank to assess potential nucleic acid and amino acid interactions (genotoxic risk) and investigate the molecular mechanism underlying DNA damage and OS modulation, respectively. Together, these targets provide complementary insights into genomic safety and redox regulation. The 3D structure of NN–VLD was downloaded from the PubChem database (https://pubchem.ncbi.nlm.nih.gov/). Before docking, the selected protein model was pre-processed to eliminate water molecules, heteroatoms, and co-crystallized ligands, followed by adding hydrogen atoms. The energy minimization of the ligand was performed using a defined force field (MMFF94), with the torsion bonds set to be rotatable for flexible docking.

The docking protocol was validated by redocking the co-crystallized ligands Netrospin and 1VV((1S,2R)-2-[(1S)-1-[(1,3-dioxoisoindol-2-yl)methyl]-3,4-dihydro-1H-isoquinoline-2 carbonyl] cyclohexane-1-carboxylic acid), which were extracted from their protein-binding pockets and re-docked with their respective proteins to get a Root Mean Square Deviation (RMSD) value of 0.50 and 1.15, respectively. We evaluated docking accuracy by calculating

the RMSD between the experimental and re-docked ligand conformations. Subsequently, NN–VLD was docked into the validated active site using the same docking parameters for both proteins with coordinates of X: 10.24, Y: 23.63, Z:72.62, a grid box of 20 Å × 20 Å × 28.7Å for 121D, and coordinates X: -3.6, Y: 2.5, Z: -27.5, a grid box of 17.5 Å × 18.1 Å × 18.3Å for 4L7B. The GeinDock scoring function was used to calculate binding affinities (kcal/mol), ligand orientation, and protein-ligand interactions, considering electrostatic, hydrogen bonding, and van der Waals interactions. The interaction profile of each complex was analyzed using BIOVIA Discovery Studio Visualizer 2024, including bond distances, angles, and interacting residues. These profiles included hydrogen bonds (≤3.5 Å cut-off), hydrophobic interactions, pi-stacking, and other non-bonded interactions.

2.2.2 Synthesis of N-Nitroso vildagliptin impurity (NN-VLD, Scheme 1)

VLD (3.5 g, 0.0109 mol) was dissolved in a mixture of acetic acid (18 mL) and water (35 mL) to form reaction mixture 1 (RM-1). A solution of sodium nitrite (1.128 g, 0.0163 mol) was added dropwise to RM-1 at 0°C under constant stirring for 30 min, affording RM-2. Subsequently, RM-2 was stirred for 2 h at 25- 30°C, and the reaction progress was monitored by TLC (**Scheme 1**). The excess nitrite was quenched with aqueous sulfamic acid, then neutralized with sodium bicarbonate. The resulting reaction mixture was washed with ethyl acetate, and the organic layer was filtered to obtain NN-VLD. The purity of the NN-VLD was evaluated using HPLC and found to be 99.38% (**Figure S1**). Structural confirmation was achieved using FTIR, ^{1}H NMR, ^{13}C NMR, and mass spectrometric analysis (**Figures S2-S5**).



Scheme 1: N-nitroso vildagliptin impurity (NN-VLD) synthetic scheme.

The spectral data for NN-VLD were consistent with the proposed structure. NN-VLD was obtained as a white crystalline solid (yield: 97%,1.0g), FTIR (cm^{-1}): 3292.97 (N-H), 2992.09-2848.60 (C-H), 1450 (N=O), 1249- 1051 (C-N), 1033.37 (C-O). ^{1}H NMR (400 MHz, DMSO-d6) δ ppm: 4.688-4.737 (2H, m), 4.318-4.446 (2H, m), 3.694-3.735 (1H, m), 3.507-3.569 (1H, m), 2.288 (2H, m), 2.127-2.160 (2H, m), 2.004-2.081 (2H, m), 1.965 (6H, s), 1.590-1.660 (4H,

m), 1.498-1.555 (2H, m), ^{13}C NMR (400 MHz, DMSO-d6) δ ppm:173.85, 170.19, 170.05, 67.71, 59.51, 58.75, 58.75, 52.61, 50.16, 45.53, 44.43, 42.81, 41.11, 35.11, 30.25, 29.29, 24.08, 22.14, mass found to be $[M+H]^+$ 333.3.

The environmental impact of the synthesis was assessed using the Analytical Eco-Scale (AES) method (*18*). The synthesis scored 79, indicating an acceptable environmental profile at the laboratory scale. This favourable rating reflects mild reaction conditions, inexpensive reagents, and a straightforward workup protocol, as shown by the relevant penalty points in **Table S1**.

2.2.3 Cell culture preparation and cell maintenance

The National Centre for Cell Science, Pune, India, provided the HepG2 cell line. We chose it as an *in vitro* model because it grows steadily and is widely used in cytotoxicity and genotoxicity studies (*19*). HepG2 cells were cultured in a T25 tissue culture flask (SPL, Korea) and maintained them in DMEM supplemented with 10% FBS and 1% antibiotic-antimycotic solution. The cells and culture medium were incubated at 37°Cin a 5% CO2 atmosphere. We checked cell morphology and confluency regularly using an inverted microscope. The culture medium was changed every 24 hr to supply fresh nutrients and remove accumulated metabolic waste for better cell growth. After reaching 70-80% confluence, cells were washed and detached with trypsin-EDTA for sub-culturing. We performed the experimental procedures on healthy, contamination-free cells in the logarithmic phase.

2.2.4 Cytotoxicity potential assessment

The cytotoxicity of NN-VLD was estimated using the widely employed MTT assay (*20*). Briefly, 1×10^5 cells/well were plated and allowed to attach for 24 hr before the experiment. After incubation, wells were treated with NN-VLD concentrations ranging from 5 to 125 µg/mL and incubated for an additional 24 hr. After 24 hr incubation, cells were supplemented with 10 µL of MTT solution (12 mM) and incubated for an additional 4 hr at controlled conditions. After removing the culture medium, formed formazan crystals were dissolved in 50 L DMSO and incubated for 60 min. Absorbance was recorded, and results were expressed as % cell viability v/s concentration. Cells in culture medium alone served as the control.

2.2.5 Preparation of NN-VLD- treated HepaG2 cell lysates

To perform the oxidative/ nitrosative stress biomarker study, NN-VLD-treated cell lysates were prepared. After 24 h of treatment with different concentrations of NN-VLD, wells were washed with ice-cold PBS to remove residual compound or medium. Add chilled lysis buffer (e.g., phosphate buffer containing protease inhibitors) to disrupt cells and extract intracellular proteins. Cells were scraped, transferred into microcentrifuge tubes, and centrifuged at 12,000

× g for 15 min at 4°C. The supernatant was carefully collected without disturbing the pellets. The protein amount of each lysate was measured by the Bradford assay (mg/mL). Enzyme activity was preserved by performing all the steps on ice.

2.2.6 Antioxidant Défense Markers

The dose-dependent effect of NN-VLD (cell lysates) on antioxidant biomarkers were studied using available literature and standard assay kits.

2.2.6.1 SOD assessment

The activity of the SOD enzyme in cells was studied using a protocol available in the literature (*21,22*) with a minor modification. The reaction mixture contained 50 mM sodium carbonate buffer (pH 10.2), EDTA (0.1 mM), nitro blue tetrazolium (NBT, 24 µM), 1 mM hydroxylamine hydrochloride ($NH_2OH \cdot HCl$), and 0.05% Triton X-100, equilibrated at ambient temperature before cell lysate addition. After adding cell lysate, we monitored NBT reduction inhibition spectrophotometrically at 560 nm at 60 Sec intervals for 2 min. The results were normalized to the total protein concentration (mg/mL) of each cell lysate to minimize variation that occurs due to differences in cell density and expressed as U/mg protein using Equation 1 (dilution factor =1).

$$\text{SOD(U/mg protein)} = \text{SOD(µM)/Total protein} \quad \ldots \textbf{Equation 1}$$

SOD (µM) levels were determined using a CC prepared from serial dilutions of standard SOD (0-10 µM), yielding the linear equation y = 0.0116x + 0.001 (**Fig.S6**). Using **Equation 2**, the concentration of SOD(µM) was determined.

$$\text{SOD(µM)} = \text{OD} + 0.001/0.0116 \quad \ldots \textbf{Equation 2}$$

2.2.6.2 Catalase (CAT) assessment

Catalase (CAT) activity was assessed by quantifying H_2O_2 decomposition, according to established protocols (*6,23*) ,with appropriate modifications. The reaction mixture consisted of phosphate buffer (pH 7.4), H_2O_2, and cell lysate, while a corresponding reaction without H_2O_2 was used as the sample blank to correct for background absorbance. The decrease in absorbance due to H_2O_2 decomposition was monitored spectrophotometrically at 240 nm at 30 Sec intervals for 2 min. CAT activity was determined from the rate of H_2O_2 decomposition, based on the change in absorbance, using the molar extinction coefficient of H_2O_2 (0.071 mM^{-1} cm^{-1}), and activity was normalized to the protein content of each cell lysate. The results were expressed as µM of H_2O_2 decomposed min^{-1} mg^{-1} protein.

2.2.6.3 Reduced Glutathione (rGSH) Estimation

The rGSH level in NN-VLD treated cell lysates was measured using the available protocol in the literature (*24,25*). The standard solutions of rGSH (L-glutathione) were prepared (1–500 μM) in water and used to construct a calibration curve. The corresponding regression equation (y = 0.0006x + 0.1196) was used to calculate the rGSH concentration (μM) in the cell lysates shown in **Fig.S7**. To assess intracellular rGSH concentration, cell lysate (100 μL) was mixed with 0.1 M phosphate buffer (100 μL, pH 7.4), 50 μL of 10 mM DTNB, and an appropriate volume of water and incubated at ambient temperature for 10 min in dark. Absorbance of each concentration was measured at 412 nm using a spectrophotometer. The obtained rGSH levels were normalized to TPC (mg/mL) using **Equation 3** and expressed as μM/mg of protein.

$$\text{rGSH (}\mu\text{Mol/mg protein)} = \text{rGSH}(\mu\text{M})/\text{Total protein} \quad \ldots \textbf{Equation 3}$$

2.2.6.4 Nrf2 assessment

The modulation of Nrf2 response in cell lysates following NN-VLD treatment was assessed using an ELISA-based double-antibody assay (GENLISA Human NRF2 kit; Cat. No. KBH 14002, Krishgen Biosystems, Mumbai, India), according to the manufacturer's standard protocol. The optical density (OD) of the samples was measured spectrophotometrically at 450 nm. Nrf2 concentrations were determined using a calibration curve generated from known concentrations of the NRF2 standard (**Fig.S8)**. The calibration curve yielded the equation *y* = 0.2359x + 0.1577, where y represents the measured OD and x represents the Nrf2 concentration (ng/mL), with a correlation coefficient (R^2) of 0.9826. The Nrf2 concentration in each sample was subsequently calculated using the equation as follows:

$$\text{Nrf2} = \frac{\text{OD}}{0.2359} - 0.1577 \quad \ldots \textbf{Equation 4}$$

2.2.7 Oxidative/Nitrosative Marker Evaluation

2.2.7.1 Determination of MDA-TBA (Thiobarbituric acid) adduct assessment

Lipid peroxidation in the cell lysate was assessed by determining MDA content using a previously reported method (*26,27*). A stock solution of 1,1,3,3-Tetramethoxypropane (TMP, a standard equivalent to MDA) was prepared and serially diluted (1 to 300 μM) to construct a calibration curve. For the test samples, combine cell lysate (200 μL) with sodium dodecyl sulphate (SDS, 8.1% (w/v), 100 μL). Later, glacial acetic acid (750 μL,20% AcOH), thiobarbituric acid (750 μL, TBA (0.8% w/v)), and distilled water were added sequentially and mixed thoroughly by vortexing to ensure proper homogenization**.** The homogenised mixture was then incubated at 100°C for 60 min to allow formation of the red-pink colour MDA-TBA adduct. After MDA-TBA adduct formation, the mixture was centrifuged, and the obtained

supernatant was carefully collected for spectrophotometric analysis. The OD of the MDA-TBA adduct was recorded at 532 nm. The corresponding MDA concentration was obtained from the TMP calibration curve (**Fig. S9**) by rearranging the calibration-curve regression equation (**Equation 5**). The resulting MDA concentration was subsequently normalized against the total protein content of the respective cell lysate and expressed as μM MDA/mg protein using **Equation 6** (*28,29*).

$$\mathrm{MDA}(\mu\mathrm{M}) = \mathrm{OD} - 0.0507/0.001 \quad \ldots\ldots \textbf{Equation 5}$$

$$\mathrm{MDA}(\mu\mathrm{Mole/mg\ of\ protein}) = \mathrm{MDA}(\mu\mathrm{M})/\mathrm{Total\ protein} \quad \ldots\ldots \textbf{Equation 6}$$

2.2.7.2 Nitric oxide determination using iNOS enzyme level

Nitric oxide (NO), a key reactive nitrogen species (RNS) is synthesized from L-arginine by NADPH-dependent nitric oxide synthases (NOS) (*30*) . The nitrosative stress (NS) was evaluated by quantifying intracellular iNOS levels using a sandwich ELISA kit (GENLISA Human iNOS [Cat. No SKU: KBH11946; Krishgen Biosystems, Mumbai, India] from humans. The iNOS determination was carried out as per manufacturer's protocol. The level of iNOS in the respective cell lysates was quantified using a calibration curve prepared with different concentrations of the iNOS standard (0.015-10 ng/mL), as shown in **Fig.S10**, by rearranging the calibration-curve regression equation (**Equation 7**).

$$\mathrm{iNOS\ (nMol/mL)} = \mathrm{OD} - 0.0194/0.0384 \quad \ldots\ldots \textbf{Equation 7}$$

2.2.8 DNA Damage Integration Assay

The genotoxicity of NN-VLD was evaluated using the alkaline comet assay following previously reported standard protocols (*31,32*). The procedure was carried out as follows:

Slide Pre-Coating with Agarose

The slides were coated with 1% normal-melting agarose to provide a stable supporting layer for cell embedding. The coated slides were allowed to solidify at room temperature prior to sample loading.

Cell Seeding, Treatment, Harvesting and Embedding

Approximately 2×10^5 cells/mL were plated per well and incubated at 37°C for 24 hr under the defined conditions (See the cell culture preparation and cell maintenance section in methodology). Following the first incubation period, the cells were treated with NN-VLD at selected concentrations in triplicate for 24 hr. Following treatment, NN-VLD-treated cells were harvested (0.05 % trypsin-EDTA) and centrifuged. The obtained cell pellets were suspended in 0.065% low-melting agarose (LMA). The cell suspension was spread onto agarose-coated

microscopic slides and allowed to solidify. The slides were dipped in cold lysis buffer overnight to separate cellular proteins.

Electrophoresis, slide staining and analysis

Before being subjected to electrophoresis at 300 mA, washed lysed cells were transferred into electrophoresis buffer to migrate fragmented DNA toward the anode. Upon completion of electrophoresis, the slides were washed and neutralized (0.4 M Tris-HCl buffer (pH 7.5)). DNA fixation was carried out by sequential immersion in 70 % ethanol and air-dried overnight. The dried slides were placed in staining reagent (Ethidium bromide (1 µg/mL)) for 15 min prior to microscopic analysis. The migration pattern of DNA in treated cells was observed using a fluorescence microscope (Leica Microsystems SP5 II confocal microscope). Comet parameters were analyzed using ImageJ software. Dimethyl sulfoxide (DMSO) and H_2O_2 served as the solvent and positive controls, respectively.

2.2.9 Statistical Analysis

Experimental observations were derived from three independent measurements from each concentration (n=3) and presented as mean ± SD (standard deviation). Normality was evaluated using the Shapiro-Wilk test. Intergroup variability was assessed through one-way analysis of variance (ANOVA). After detecting a statistically significant difference, Dunnett's multiple comparison procedure was employed to compare each treated group against the control. Statistical significance was denoted by asterisk symbols, where * indicates $p < 0.05$, ** $p < 0.01$, and *** $p < 0.001$. Statistical analysis and graphical representations were performed using GraphPad Prism software (version 8.1.0).

3 RESULTS AND DISCUSSION

3.1 Chemistry of NN-VLD

Targeted compound **(2**) was synthesized via a single-step approach starting from commercially available compound (**1**). The synthetic route is outlined in **Scheme 1.** The N-[2-[(2S)-2-cyanopyrrolidin-1yl]-2-oxoethyl-N-[(5S,7R)- 3-hydroxy-1-adamantyl] nitrous amide (**2**) was synthesized by nitrosation of (2S)-1-[2-[(3-hydroxy-1-adamantyl) amino] acetyl] pyrrolidine-2-carbonitrile (**1**) under mild acidic (Acetic acid) conditions. In the presence of acetic acid and water, sodium nitrite generates nitrous acid (HNO_2), which subsequently equilibrates to form highly electrophilic nitrosonium ion (NO^+). The reaction was carried out at a low temperature (0-5°C). After workup and purification, compound **2** was isolated in 97% yield, whereas an earlier study reported 75% yield (*33*). The obtained compound **2** was confirmed by FTIR spectrum, which exhibited characteristic absorption bands attributed to N–H stretching

(3293 cm^{-1}), N=O stretching (1450 cm^{-1}), and C–N stretching (1033 cm^{-1}). The ^{1}H NMR spectrum displays signals consistent with aliphatic protons and the protons of the adamantane moiety, while ^{13}C NMR confirmed the expected carbon environment. Mass spectrometry confirmed a molecular ion peak ($C_{19}H_{24}N_4O_3$) consistent with the calculated molecular weight.

3.2 Molecular Docking Analysis

A molecular docking study was performed to evaluate the binding potential of NN- VLD against a DNA helix and the NRF2-KEPA1 protein. The docking of co-crystallised ligand 1VV with 4L7B and NT with 121D yielded binding energies (BE) of -10.35kcal/mol and -10.80 kcal/mol, respectively. 1VV reproduced key interactions with residues located within the binding cavity, including Arg415, Asn414, Ser602, Ala556, Tyr572, and Tyr334 (**Fig.1**), while NT reproduced interactions with DT: A8, DT: A9, DA: B18, DT: A7, DA: A6, DG: B22, DT: B20, DT: B21(**Fig.2**), consistent with the crystal structure. NN-VLD (-8.67kcal/mol) displayed a favourable BE with 4L7B protein comparable to the co-crystallised ligand(1VV) and made stable interactions with Arg415, Asn414, Ser602, Ala556, Ser602, and Tyr334 (**Fig.3**), crucial for NRF2 activation. With the DNA helix, NN-VLD binds with a BE of -7.88kcal/mol compared to the co-crystallised ligand (NT) and displays favourable residual binding with DG: B22, DT: B20, DT: B21 (**Fig .4**).

Molecular docking suggests that NN-VLD shows favourable binding with both the Keap1 protein and DNA helix. NN-VLD exhibited a lower BE toward Keap1 (4L7B) than the co-crystallised ligand (1VV), suggesting that NN-VLD may have the capacity to associate with the Keap1 binding pocket and potentially modulate the Keap1-Nrf2 pathway. Against DNA, NN-VLD also exhibited a lower BE than the co-crystal ligand (NT) and established non-covalent interactions with guanine and thymidine. This finding indicates a potential DNA-binding propensity. However, the weaker affinity relative to the reference ligand suggests that NN-VLD does not interact with DNA as strongly as NT under the applied docking conditions. Collectively, the docking results support NN- VLD's potential to interact with Keap1 and DNA, warranting further investigation through in vitro studies.

3.3 Cytotoxicity evaluation assay

The cytotoxic potential of NN- VLD was evaluated using the MTT assay over a concentration range of 5-125 µg/mL. Cell viability in the control group was 100%, whereas treatment with 5- 25 µg/mL reduced it to 61.47- 51.32% ($p < 0.01$). A pronounced reduction in viability was observed at 50-125 µg/mL, with survival rates of approximately 22.29- 19.10% ($p < 0.001$,

Fig.5). These findings clearly demonstrated a statistically dose-dependent cytotoxic effect of NN-VLD, with an estimated IC_{50} of 19.27 µg/mL shown in **Table S2**.

3.4 Antioxidant Biomarkers Evaluation

3.4.1 NN-VLD-Induced Alteration of SOD Activity

The effect of NN-VLD on cellular SOD activity following 24 h exposure is presented in **Table S3** and **Fig. 6A**. NN-VLD treatment showed a significant decrease in SOD activity at concentrations of 50-125 µg/mL (p<0.001), whereas no significant change in SOD activity was observed at 5-25µg/mL compared with the untreated control. The reduction in SOD activity with increasing NN-VLD exposure suggests disruption of the cellular antioxidant defence system. SOD is a key antioxidant enzyme that eliminates superoxide radicals. Its significant reduction at 50-125 µg/mL of NN-VLD may suggest that oxidative burden becomes sufficient to impair the antioxidant defence system. No significant SOD effect at 5-25 µg/mL may indicate that basal antioxidant capacity is sufficient to maintain redox homeostasis at relatively low NN-VLD concentrations. Decreases in SOD accompanied by increases in ROS and MDA have been reported following nitrosamine exposure in HepG2 cells, supporting OS as a contributor to nitrosamine-induced genotoxicity (*14*) . Nitrosamines have also been shown to induce ROS and DNA damage, which can be attenuated by antioxidants (*34*). These findings support oxidative imbalance as a possible mechanism of NN-VLD-induced cellular injury.

3.4.2 Catalase (CAT) Activity

Table **S4 and Fig. 6B** present CAT activity after 24 h exposure to NN-VLD. NN-VLD treatment showed a concentration-dependent reduction in CAT activity. No significant change in CAT activity was observed at 5-75 µg/mL. However, CAT activity was significantly decreased at 100 and 125 µg/mL ($p < 0.05$) compared with the control group, indicating that higher concentrations of NN-VLD adversely affect the cellular antioxidant defence system. CAT enzyme catalyzed the conversion of H_2O_2 into water and oxygen, thereby limiting H_2O_2 accumulation and oxidative damage. The significant reduction in CAT activity suggests impaired H_2O_2-scavenging capacity and disturbance of cellular redox homeostasis at higher NN-VLD exposure.

3.4.3 Reduced glutathione (rGSH) enzyme Study

The results presented in **Table S5** and **Fig. 6C** show that treatment with NN-VLD significantly decreases intracellular rGSH levels at 50-100 µg/mL ($p < 0.05$), whereas no significant alteration was observed at 5, 25, and 125µg/mL. This concentration-dependent depletion of rGSH suggests disruption of cellular redox homeostasis at higher NN-VLD concentrations.

GSH is a major antioxidant (non-enzymatic), maintains intracellular thiol redox balance, participates in ROS detoxification through the glutathione-dependent antioxidant pathway (*35*). Similar GSH depletion and oxidative stress have been reported following nitrosamine exposure (*14,36*). Thus, NN-VLD-induced rGSH depletion may contribute to oxidative imbalance and potentially to genotoxic effects.

3.4.4 Nrf2 activation pathway

NRF2 protein levels in respective cell lysates were evaluated following 24 h treatment with NN-VLD. As shown in **Fig. 6D** and **Table S6**, NN-VLD treatment produced a significant reduction in NRF2 protein level at 100-125 µg/mL ($P < 0.05$ and < 0.01, respectively). Whereas no significant changes were observed at 5-75µg/mL. These findings indicate that higher concentrations of NN-VLD may affect the cellular Nrf2-mediated antioxidant response. Nrf2 is a central transcriptional regulator of cellular antioxidant and cytoprotective responses and regulates the expression of multiple genes involved in maintaining redox homeostasis (*37*). Reduced Nrf2 protein levels suggest attenuated cellular antioxidant defences following high NN-VLD exposure.

3.5 Oxidative/ Nitrosative Marker Evaluation

3.5.1 MDA analysis

Lipid peroxidation was assessed by measuring MDA, a major secondary product of polyunsaturated fatty-acid oxidation and a commonly used marker of oxidative damage (*29,38*). As shown in **Table S7** and **Fig. 7A**, NN-VLD treatment produced a concentration-dependent increase in MDA levels, with significant elevations observed at all tested concentrations except 5 µg/mL ($p < 0.05$, $p < 0.01$ and $p < 0.001$). The progressive increase in MDA indicates enhanced lipid peroxidation following NN-VLD exposure and supports oxidative stress at higher concentrations.

3.5.2 iNOS Analysis

The effect of NN-VLD treatment on iNOS expression was evaluated following 24 h exposure in cells. As shown in **Table S8** and **Fig. 7B**, iNOS expression was significantly downregulated at the tested concentrations of 5-75µg/mL ($p < 0.001$, $p < 0.01$, and $p < 0.05$, respectively) compared with the control group and no significant change was observed at 100-125µg/mL. This consistent reduction indicates that NN-VLD exposure did not increase iNOS expression under the present experimental conditions. Direct measurement of NO levels is difficult, so in the current study we measured the enzyme iNOS, which catalyses the production of nitric oxide (NO), which can react rapidly with superoxide radical to generate peroxynitrite ($ONOO^-$), a

potent oxidant capable of inducing oxidative damage to cellular proteins, lipids and DNA (*39*). Therefore, the observed downregulation of iNOS does not support the increase in iNOS-mediated NO production as a major contributor to NN-VLD-induced oxidative injury.

3.6 DNA Integrity Measurement

The genotoxic potential of NN-VLD was assessed using a commonly used technique. The alkaline comet assay is a highly sensitive method for effectively detecting DNA damage. The assay measures % tail DNA, tail intensity (TI), olive moment (OM), and % head DNA as key indicators that correlate with the extent of DNA damage (*40*). Hydrogen peroxide (H_2O_2), used as a positive control, interferes with DNA repair and enhances baseline DNA damage (*41*), leading to higher tail intensity, % tail DNA, and OM. Our findings are consistent with this principle, the positive control showed significant induction in tail intensity, % tail DNA and OM ($p<0.001$) and significant reduction in % head DNA ($p<0.001$). Increased tail intensity indicates more DNA strand breaks, as fragmented DNA migrates toward the tail region during electrophoresis (*42*). The selected DNA damage parameters were analyzed using ImageJ software, and results are shown in **Table 1**. Thus, a higher tail intensity corresponds to DNA damage. Our findings are consistent with this principle.

A comparison of the % head DNA and % tail DNA of all tested concentrations of NN–VLD with the solvent control, statistically depicted in **Fig. 8**, shows a significant decrease in % head DNA ($p < 0.05$, **Fig.8A**) and a significant increase in % tail DNA ($p <0.05$, **Fig.8B**) at 125 µg/mL compared with the solvent control, indicating mild DNA migration towards the tail region. While other concentrations were observed, no significant changes in % head and tail DNA.

On the other hand, no significant changes were observed in the % tail intensity (**Fig.7C**) and OM (**Fig.7D**) of all tested concentrations of NN-VLD. The morphological images for each concentration at 25µm are shown in **Fig. 9**. The *in vitro* comet assay results were consistent with in silico molecular docking findings with DNA, supporting that NN–VLD did not produce substantial or consistent DNA strand breaks.

5. CONCLUSION

The present study provides an integrated evaluation of the compound-specific cellular toxicological effects of NN-VLD, encompassing cytotoxic, biochemical, DNA-integrity, and *in silico* investigations. NN-VLD exhibited pronounced concentration-dependent cytotoxicity, accompanied by alterations in cellular redox homeostasis. Reductions in SOD, CAT, and

rGSH, together with increased MDA formation, indicate impairment of both enzymatic and non-enzymatic antioxidant defences, inducing substantial oxidative stress and enhanced lipid peroxidation. The concomitant reduction in Nrf2 observed at the highest concentrations further suggests attenuation of the cellular antioxidant response under conditions of increased cellular stress.

NN-VLD did not induce iNOS expression; instead, it downregulated iNOS at lower and intermediate concentrations and left it unchanged at higher concentrations. Thus, the biochemical findings of NN-VLD clearly perturb antioxidant defence and redox homeostasis, with enhanced lipid peroxidation rather than activation of an iNOS-driven nitrosative-stress pathway. Despite the marked biochemical alterations, the DNA response was comparatively limited. Significant alterations in % tail DNA and % head DNA were observed only at the highest NN-VLD concentration, whereas the remaining comet parameters were not significantly affected. These findings indicate that NN-VLD did not produce substantial or consistent DNA strand breaks. Although the limited DNA changes observed at high exposure occurred alongside pronounced redox imbalance, these findings do not establish a direct causal relationship between oxidative stress and DNA damage.

The *in-silico* findings complemented the cellular observations by showing that NN-VLD can form favourable predicted interactions with both the Keap1 binding site and the DNA duplex. Although its predicted binding energies were weaker than those of the respective reference ligands, these interactions provide a supportive structural basis for potential association with Keap1/Nrf2 and DNA. Nevertheless, interpret the docking results as complementary mechanistic evidence rather than direct proof of pathway modulation, DNA binding, or genotoxicity.

Overall, the findings establish a multilevel toxicological response to NN-VLD, with cytotoxicity accompanied by progressive impairment of antioxidant defence, enhanced lipid peroxidation, and alteration of Nrf2 signalling. The absence of induced iNOS expression and the limited DNA migration response suggest that, under the conditions examined, redox imbalance represents a more prominent feature of NN-VLD-induced cellular toxicity than iNOS-mediated nitrosative response or substantial DNA damage. These findings contribute to the limited toxicological understanding of NN-VLD and provide a mechanistic basis for further investigation using direct ROS/NO measurements, Nrf2-regulated molecular endpoints, complementary genotoxicity assays, and metabolically competent systems to clarify its toxicological significance.

6. FUTURE PROSPECTIVE

The present findings establish how NN-VLD mechanistically induced redox disturbance relates to cellular and genomic responses. Future studies should clarify whether NN-VLD-induced redox imbalance results from direct ROS generation by assessing intracellular ROS, mitochondrial oxidative stress, and Keap1-Nrf2 signalling. The limited DNA response observed at high NN-VLD exposure warrants mechanistic discrimination between general DNA strand-break formation and oxidative DNA lesions. Future studies should incorporate lesion-specific endpoints. Using metabolic activation systems and metabolically competent models would further clarify whether NN-VLD or its biotransformation products drive the observed responses. Collectively, these investigations could move the current evidence from an association between NN-VLD exposure and redox disturbance toward a mechanistically resolved model distinguishing cytotoxic, oxidative, nitrosative, and genotoxic pathways. Such an approach would provide a stronger scientific basis for defining the toxicological significance and safety profile of NN-VLD as an NDSRI.

DECLARATION OF COMPETING INTERESTS

The authors declare that they have no financial or personal relationships that may have influenced the work reported in this manuscript

ACKNOWLEDGEMENTS

The authors would like to express their heartfelt gratitude to the management of Dr Vishwanath Karad MIT World Peace University, Kothrud, Pune 411038, for their support and for providing excellent infrastructure, which greatly facilitated the completion of this work.

FUNDING

This research received no specific grant from funding agencies.

DATA AVAILABILITY

Data are available in the article supplementary material.

REFERENCES

1. Jakszyn P. Nitrosamine and related food intake and gastric and oesophageal cancer risk: A systematic review of the epidemiological evidence. World J Gastroenterol. 2006;12(27):4296. doi:10.3748/wjg.v12.i27.4296
2. Aishwarya D, Ramakant Dhampalwar V, Pallaprolu N, Peraman R. Nitrosamine Drug Substance-Related Impurities (NDSRIs) in Pharmaceuticals: Formation, Mitigation Strategies, and Emphasis on Mutagenicity Risks. Pharm Res. 2025 Apr 23;42(4):547–78. doi:10.1007/s11095-025-03857-9
3. Ristic S, Byiers S, Foley J, Holmes D. Improved glycaemic control with dipeptidyl peptidase-4 inhibition in patients with type 2 diabetes: vildagliptin (LAF237) dose

response. Diabetes Obes Metab. 2005 Nov;7(6):692–8. doi:10.1111/j.1463-1326.2005.00539.x

4. Lauster CD, McKaveney TP, Muench S V. Vildagliptin: A novel oral therapy for type 2 diabetes mellitus. American Journal of Health-System Pharmacy. 2007 Jun 15;64(12):1265–73. doi:10.2146/ajhp060564

5. Kumar V, Balthu L, Pepakayala S, Lohia YK, Kathuria D, Mathur P, et al. N-Nitroso-Vildagliptin, A New N-Nitrosamine Drug Substance Related Impurity (NDSRI) of Vildagliptin- An Antidiabetic Drug: Synthesis, Characterization and Development of Sensitive LC–MS/MS Method. Chromatographia. 2025 Oct 12;88(10):791–9. doi:10.1007/s10337-025-04437-0

6. Giri P, Chabukswar A, Waghmare P, Raut K. Synthesis and Toxicological Evaluation of N-Nitroso Vildagliptin Amide Impurity in BALB 3T3 Clone Cells. Journal of Applied Toxicology. 2026 May 12;46(5):1654–66. doi:10.1002/jat.4983

7. He L, He T, Farrar S, Ji L, Liu T, Ma X. Antioxidants Maintain Cellular Redox Homeostasis by Elimination of Reactive Oxygen Species. Cellular Physiology and Biochemistry. 2017;44(2):532–53. doi:10.1159/000485089

8. Jena AB, Samal RR, Bhol NK, Duttaroy AK. Cellular Red-Ox system in health and disease: The latest update. Biomedicine & Pharmacotherapy. 2023 Jun;162:114606. doi:10.1016/j.biopha.2023.114606

9. Halliwell B, Cross CE. Oxygen-derived species: their relation to human disease and environmental stress. Environ Health Perspect. 1994 Dec;102(suppl 10):5–12. doi:10.1289/ehp.94102s105

10. Radi R. Oxygen radicals, nitric oxide, and peroxynitrite: Redox pathways in molecular medicine. Proceedings of the National Academy of Sciences. 2018 Jun 5;115(23):5839–48. doi:10.1073/pnas.1804932115

11. Arranz N, Haza AI, García A, Rafter J, Morales P. Protective effect of vitamin C towards N-nitrosamine-induced DNA damage in the single-cell gel electrophoresis (SCGE)/HepG2 assay. Toxicology in Vitro. 2007 Oct;21(7):1311–7. doi:10.1016/j.tiv.2007.03.015

12. Erkekoglu P, Baydar T. Evaluation of the protective effect of ascorbic acid on nitrite- and nitrosamine-induced cytotoxicity and genotoxicity in human hepatoma line. Toxicol Mech Methods. 2010 Feb 25;20(2):45–52. doi:10.3109/15376510903583711

13. Ma Q. Role of Nrf2 in Oxidative Stress and Toxicity. Annu Rev Pharmacol Toxicol. 2013 Jan 6;53(1):401–26. doi:10.1146/annurev-pharmtox-011112-140320

14. Dong L, Jiang Z, Yang L, Hu F, Zheng W, Xue P, et al. The genotoxic potential of mixed nitrosamines in drinking water involves oxidative stress and Nrf2 activation. J Hazard Mater. 2022 Mar;426:128010. doi:10.1016/j.jhazmat.2021.128010

15. Aktan F. iNOS-mediated nitric oxide production and its regulation. Life Sci. 2004 Jun;75(6):639–53. doi:10.1016/j.lfs.2003.10.042

16. Cinelli MA, Do HT, Miley GP, Silverman RB. Inducible nitric oxide synthase: Regulation, structure, and inhibition. Med Res Rev. 2020 Jan 13;40(1):158–89. doi:10.1002/med.21599

17. Robichová S, Slameňová D, Chalupa I, Šebová L. DNA lesions and cytogenetic changes induced by N-nitrosomorpholine in HepG2, V79 and VH10 cells: the protective effects of Vitamins A, C and E. Mutation Research/Genetic Toxicology and Environmental Mutagenesis. 2004 Jun;560(2):91–9. doi:10.1016/j.mrgentox.2004.01.011

18. Van Aken K, Strekowski L, Patiny L. EcoScale, a semi-quantitative tool to select an organic preparation based on economical and ecological parameters. Beilstein Journal of Organic Chemistry. 2006 Mar 3;2. doi:10.1186/1860-5397-2-3

19. Park SY, Choi J. Cytotoxicity, genotoxicity and ecotoxicity assay using human cell and environmental species for the screening of the risk from pollutant exposure. Environ Int. 2007 Aug;33(6):817–22. doi:10.1016/j.envint.2007.03.014

20. Horiuchi N, Nakagawa K, Sasaki Y, Minato K, Fujiwara Y, Nezu K, et al. In vitro antitumor activity of mitomycin C derivative (RM-49) and new anticancer antibiotics (FK973) against lung cancer cell lines determined by tetrazolium dye (MTT) assay. Cancer Chemother Pharmacol. 1988 Sep;22(3):246–50. doi:10.1007/BF00273419

21. Beauchamp C, Fridovich I. Superoxide dismutase: Improved assays and an assay applicable to acrylamide gels. Anal Biochem. 1971 Nov;44(1):276–87. doi:10.1016/0003-2697(71)90370-8

22. Weydert CJ, Cullen JJ. Measurement of superoxide dismutase, catalase and glutathione peroxidase in cultured cells and tissue. Nat Protoc. 2010 Jan 17;5(1):51–66. doi:10.1038/nprot.2009.197

23. Lück H. Catalase. In: Methods of Enzymatic Analysis. Elsevier; 1965. p. 885–94. doi:10.1016/B978-0-12-395630-9.50158-4

24. Salbitani G, Bottone C, Carfagna S. Determination of Reduced and Total Glutathione Content in Extremophilic Microalga Galdieria phlegrea. Bio Protoc. 2017;7(13). doi:10.21769/BioProtoc.2372

25. Anderson ME. [70] Determination of glutathione and glutathione disulfide in biological samples. In. 1985. p. 548–55. doi:10.1016/S0076-6879(85)13073-9

26. Ohkawa H, Ohishi N, Yagi K. Assay for lipid peroxides in animal tissues by thiobarbituric acid reaction. Anal Biochem. 1979 Jun;95(2):351–8. doi:10.1016/0003-2697(79)90738-3

27. Reitznerová A, Šuleková M, Nagy J, Marcinčák S, Semjon B, Čertík M, et al. Lipid Peroxidation Process in Meat and Meat Products: A Comparison Study of Malondialdehyde Determination between Modified 2-Thiobarbituric Acid Spectrophotometric Method and Reverse-Phase High-Performance Liquid Chromatography. Molecules. 2017 Nov 16;22(11):1988. doi:10.3390/molecules22111988

28. Anand SK, Sahu MR, Mondal AC. Induction of oxidative stress and apoptosis in the injured brain: potential relevance to brain regeneration in zebrafish. Mol Biol Rep. 2021 Jun 24;48(6):5099–108. doi:10.1007/s11033-021-06506-7

29. Tsikas D. Assessment of lipid peroxidation by measuring malondialdehyde (MDA) and relatives in biological samples: Analytical and biological challenges. Anal Biochem. 2017 May;524:13–30. doi:10.1016/j.ab.2016.10.021

30. Chung BH, Kim S, Kim JD, Lee JJ, Baek YY, Jeoung D, et al. Syringaresinol causes vasorelaxation by elevating nitric oxide production through the phosphorylation and dimerization of endothelial nitric oxide synthase. Exp Mol Med. 2012;44(3):191. doi:10.3858/emm.2012.44.3.014

31. Wankhade S, Nikhil P, Jain R, Mishra S, Kumarasamy M, Ramalingam P. Forced Degradation Products of Olmesartan Medoxomil and their *In Vitro* Genotoxicity Assessment by Comet Assay using HEK Cells. ChemistrySelect. 2024 May 3;9(17). doi:10.1002/slct.202400221

32. Giordani CFA, Campanharo S, Wingert NR, Bueno LM, Manoel JW, Costa B, et al. In vitro toxic evaluation of two gliptins and their main impurities of synthesis. BMC Pharmacol Toxicol. 2019 Dec 19;20(S1):82. doi:10.1186/s40360-019-0354-2

33. Kumar V, Balthu L, Pepakayala S, Lohia YK, Kathuria D, Mathur P, et al. N-Nitroso-Vildagliptin, A New N-Nitrosamine Drug Substance Related Impurity (NDSRI) of Vildagliptin- An Antidiabetic Drug: Synthesis, Characterization and Development of Sensitive LC–MS/MS Method. Chromatographia. 2025 Oct 12;88(10):791–9. doi:10.1007/s10337-025-04437-0

34. Erkekoglu P, Baydar T. Evaluation of the protective effect of ascorbic acid on nitrite- and nitrosamine-induced cytotoxicity and genotoxicity in human hepatoma line. Toxicol Mech Methods. 2010 Feb 25;20(2):45–52. doi:10.3109/15376510903583711

35. Nuhu F, Gordon A, Sturmey R, Seymour AM, Bhandari S. Measurement of Glutathione as a Tool for Oxidative Stress Studies by High Performance Liquid Chromatography. Molecules. 2020 Sep 13;25(18):4196. doi:10.3390/molecules25184196

36. Ezhilarasan D, Karthikeyan S. Silibinin alleviates N-nitrosodimethylamine-induced glutathione dysregulation and hepatotoxicity in rats. Chin J Nat Med. 2016 Jan;14(1):40–7. doi:10.3724/SP.J.1009.2016.00040 PubMed PMID: 26850345.

37. Tonelli C, Chio IIC, Tuveson DA. Transcriptional Regulation by Nrf2. Antioxid Redox Signal. 2018 Dec 23;29(17):1727–45. doi:10.1089/ars.2017.7342

38. Aguilar Diaz De Leon J, Borges CR. Evaluation of Oxidative Stress in Biological Samples Using the Thiobarbituric Acid Reactive Substances Assay. Journal of Visualized Experiments. 2020 May 12;(159). doi:10.3791/61122

39. Beckman JS, Koppenol WH. Nitric oxide, superoxide, and peroxynitrite: the good, the bad, and ugly. American Journal of Physiology-Cell Physiology. 1996 Nov 1;271(5):C1424–37. doi:10.1152/ajpcell.1996.271.5.C1424

40. Kumaravel TS, Vilhar B, Faux SP, Jha AN. Comet Assay measurements: a perspective. Cell Biol Toxicol. 2009 Feb 27;25(1):53–64. doi:10.1007/s10565-007-9043-9

41. Valverde M, Lozano-Salgado J, Fortini P, Rodriguez-Sastre MA, Rojas E, Dogliotti E. Hydrogen Peroxide-Induced DNA Damage and Repair through the Differentiation of Human Adipose-Derived Mesenchymal Stem Cells. Stem Cells Int. 2018 Oct 10;2018:1–10. doi:10.1155/2018/1615497

42. Reinecke SA, Reinecke AJ. The Comet Assay as Biomarker of Heavy Metal Genotoxicity in Earthworms. Arch Environ Contam Toxicol. 2004 Feb;46(2):208–15. doi:10.1007/s00244-003-2253-0

Figures:

Fig.1. Co-crystallized ligand (1VV) 2D and 3D interactions with 4L7B.

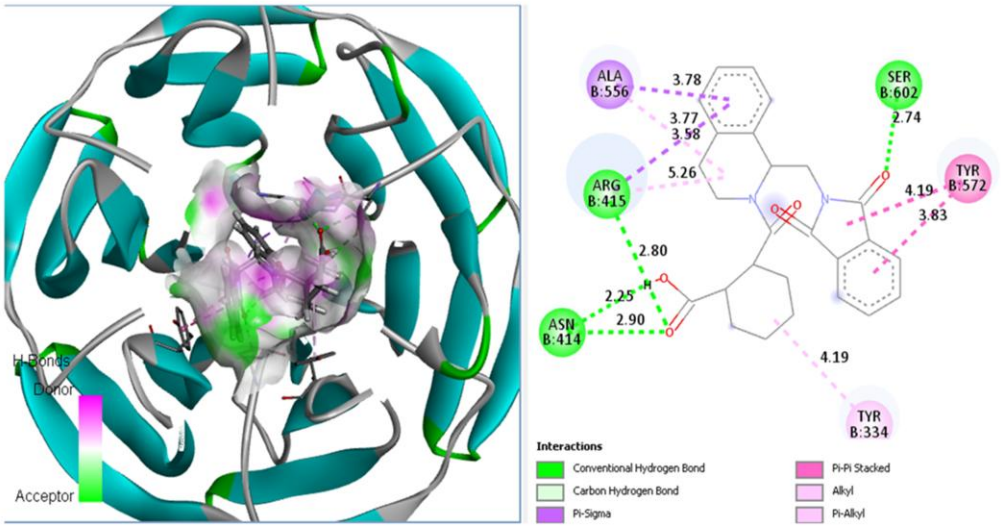


Fig.2. Co-crystallized ligand (Netrospin) 2D and 3D binding interactions with 121D.

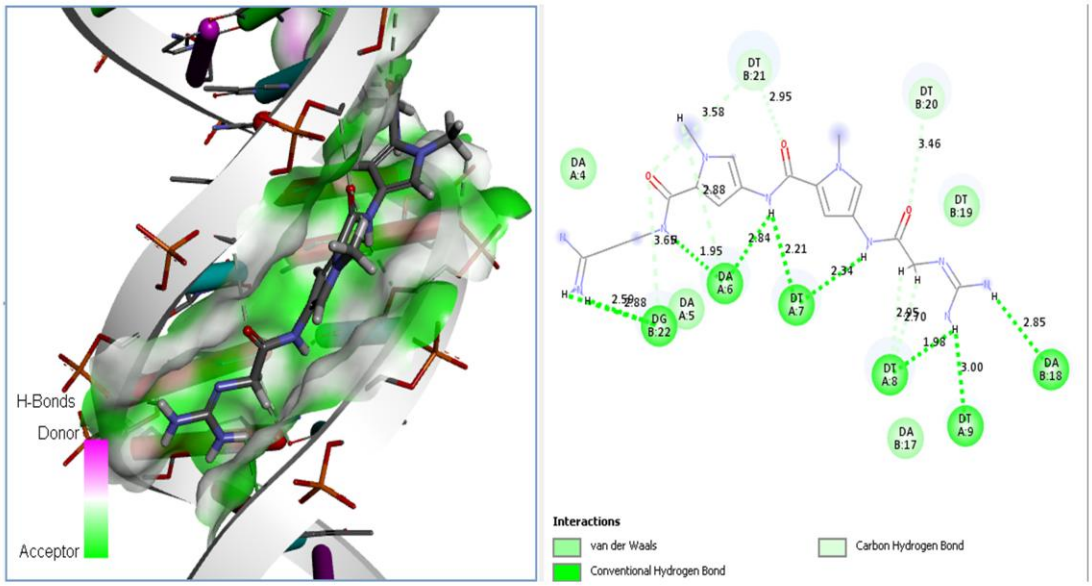


Fig.3. 2D and 3D binding interactions of NN-VLD against 4L7B.

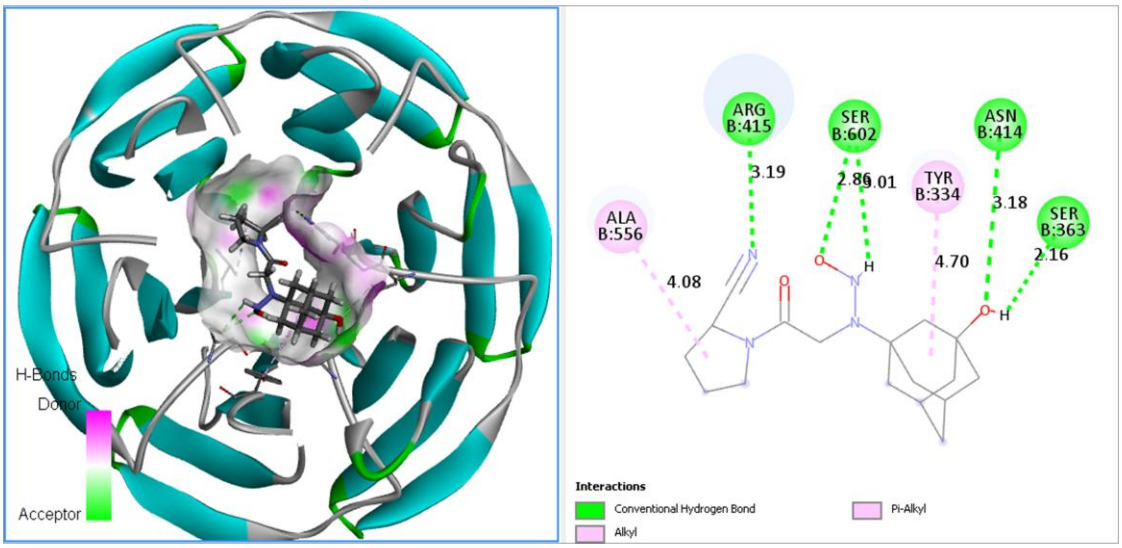


Fig.4. 2D and 3D binding interactions of NN-VLD against 121D.

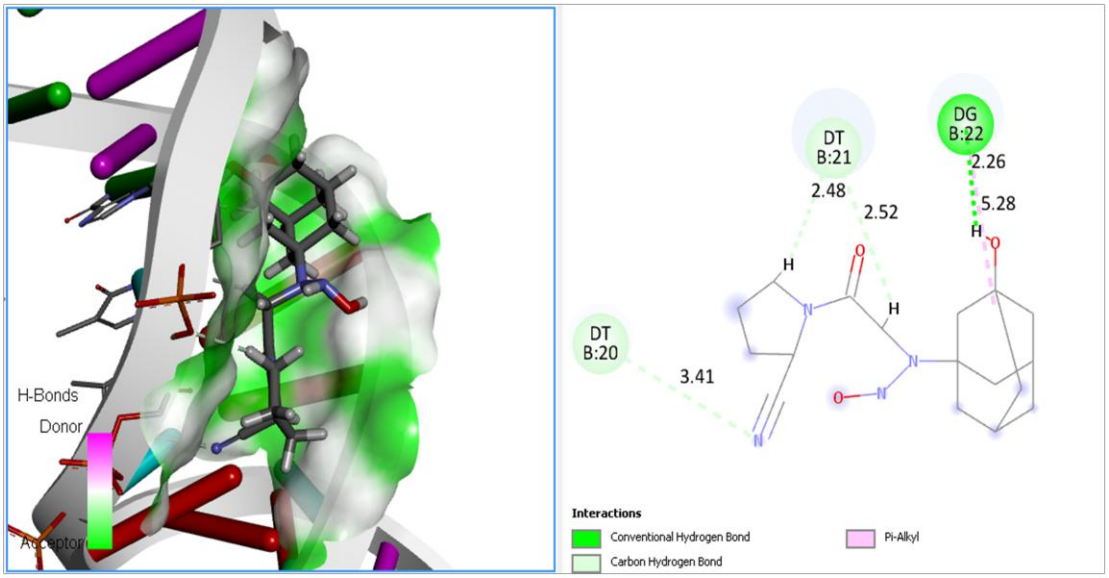


Fig.5. Effect of NN-VLD on cell viability.

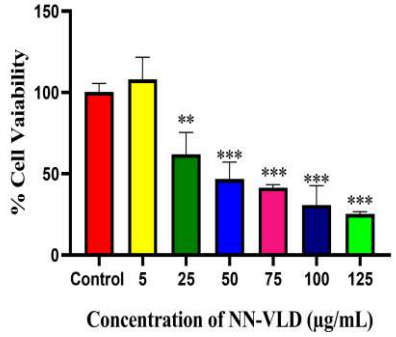


Fig.6: Effect of NN-VLD exposure on (A) superoxide dismutase (SOD) activity, (B) catalase (CAT) activity, (C) reduced glutathione (rGSH) levels, and (D) nuclear factor erythroid 2–related factor 2 (Nrf2) levels in cells.

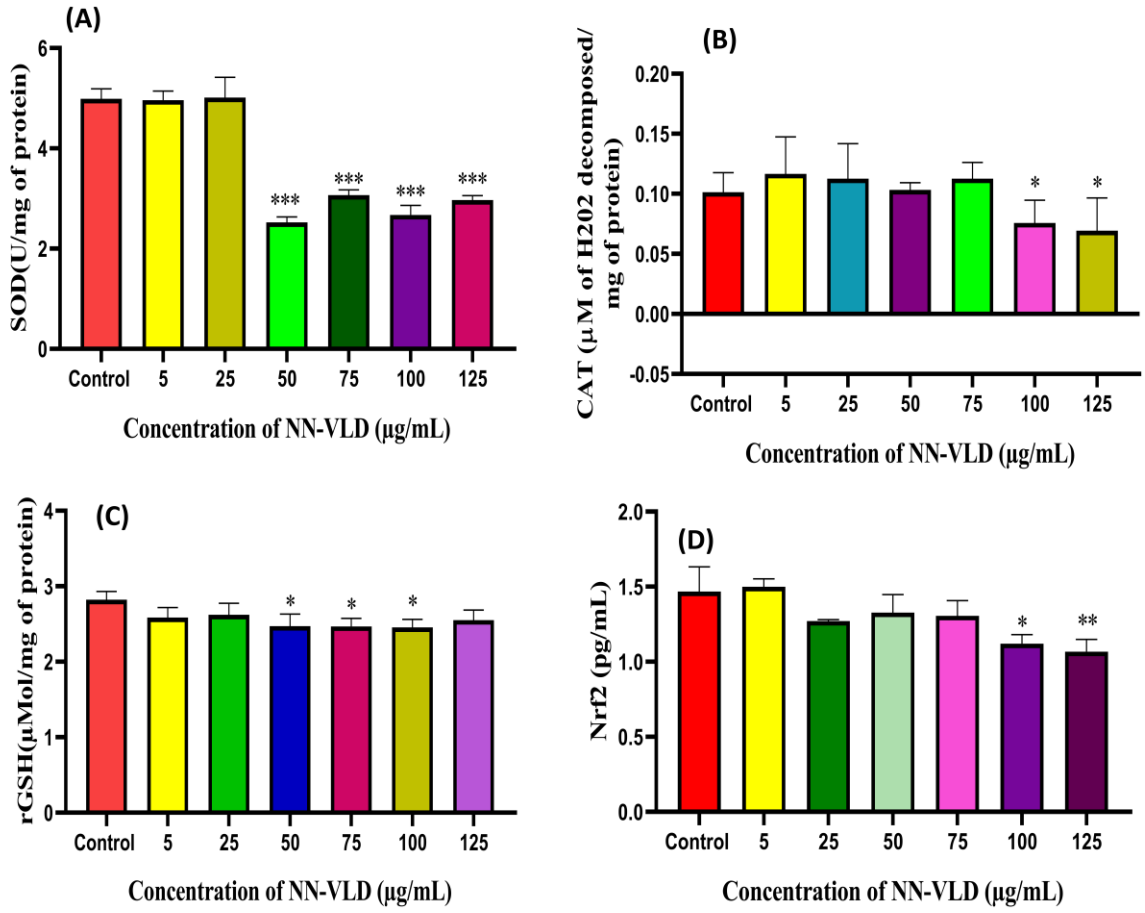


Fig.7: Alteration of (A) Lipid Peroxidation and (B) Inducible Nitric Oxide Synthase (iNOS) Response Following NN–VLD Exposure.

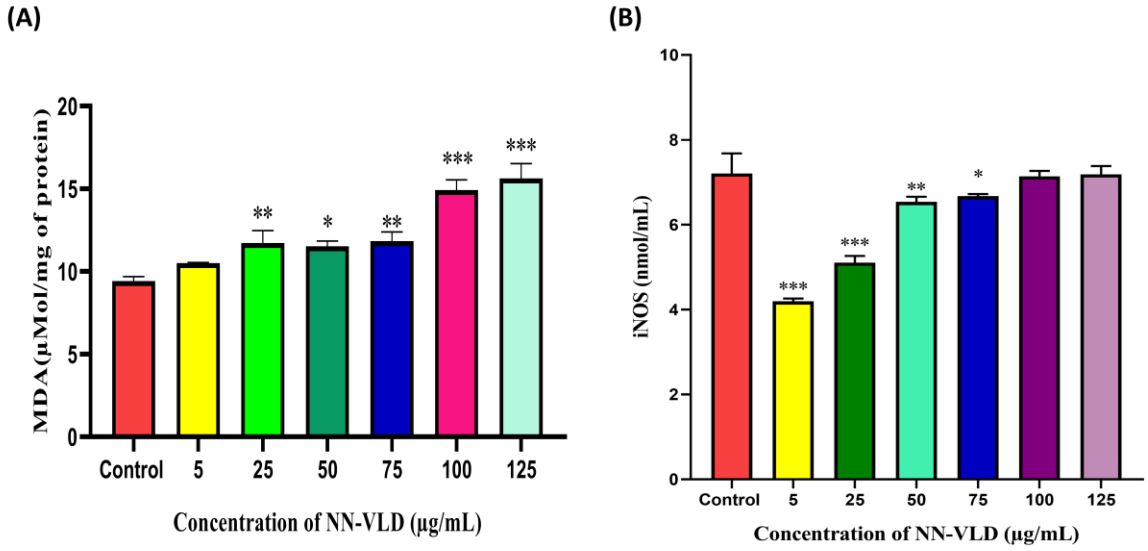


Fig.8: Comet assay-based assessment of DNA damage in treated cells. (A) Head DNA (%), (B) Tail DNA (%), (C) Tail Intensity, and (D) Olive tail moment. H_2O_2 served as the positive control, and DMSO as the vehicle control.

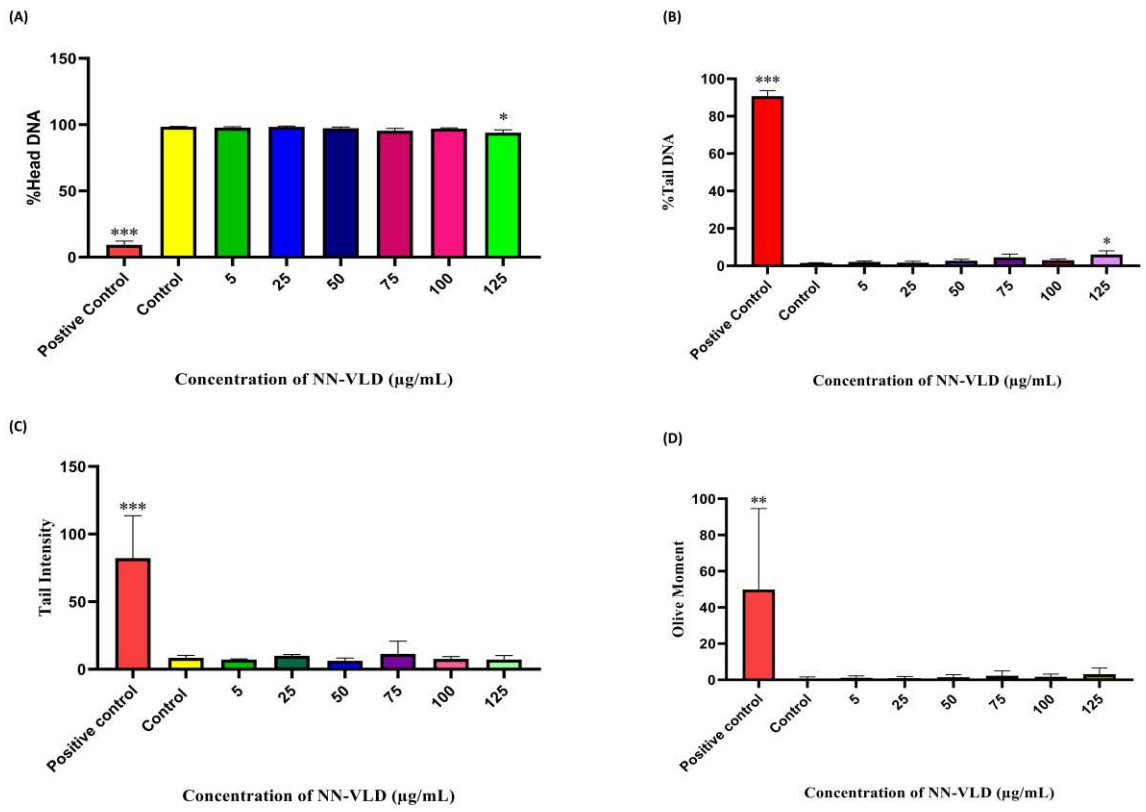


Fig.9: Fluorescence microscopy images showing DNA integrity assessment across different concentrations of N-nitroso Vildagliptin. H_2O_2 served as the positive control, and DMSO as the vehicle control.

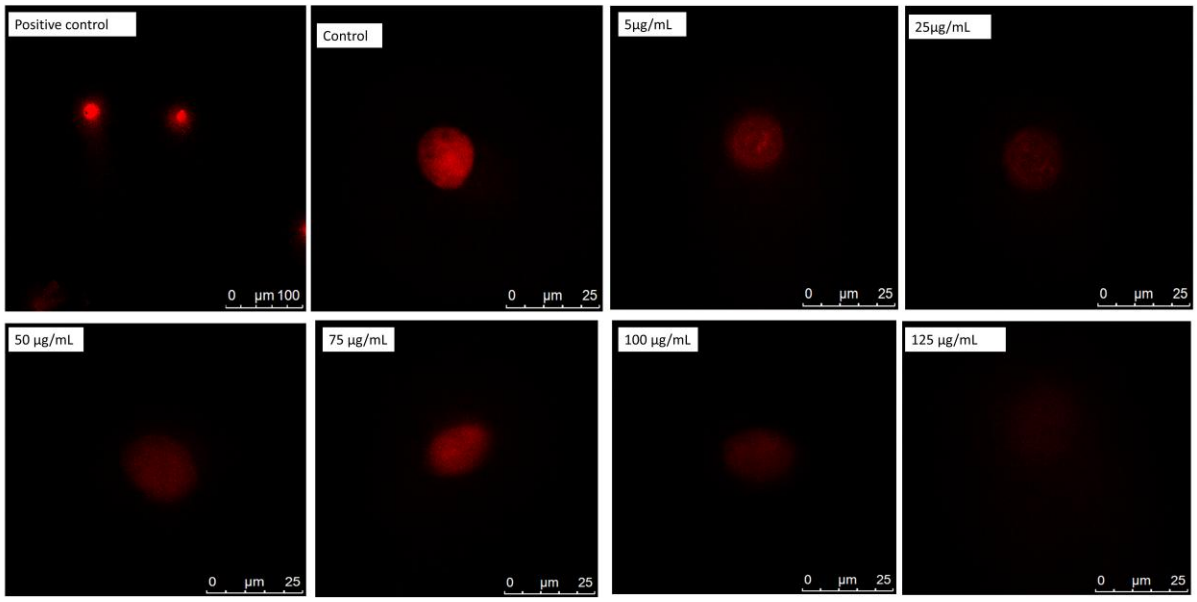


Table 1: DNA fragmentation assessment of N-nitroso vildagliptin using Comet Assay Parameters.

Supplementary Files

This is a list of supplementary files associated with this preprint. Click to download.

- Table1.docx
- Supplimentarydata.docx